COMPARATIVE ASSESSMENT OF SYNTHESIS OF ZEOLITE X FROM KANKARA AND ELEFUN KAOLINITE CLAY

[*]Ajayi, O. A.[1], Maciver, V. P.[1], Arowosaiye, M. J.[1] and Adefila, S. S.[2]

[1]Department of Chemical Engineering
Ahmadu Bello University, Zaria-Kaduna State
[2]Engineering and Environmental Management Services, Limited.
Suit 5, Plot 1469, ZM Plaza, Ahmadu Bello Way, Area 11, Abuja.
Corresponding author: aoajayi@abu.edu.ng *and* segeaj@gmail.com

ABSTRACT

Zeolite NaX was successfully synthesized from both Kankara and Elefun kaolinite clay. Both clays were wet beneficiated, calcined at 850°C for six hours, to obtain a more reactive metakaolin. The metakaolin was dealuminated using 60wt% tetraoxosulphate (VI) acid for three minutes, washed to neutrality before the introduction of calculated amount of NaOH. The resulting gels were aged for seven days at room temperature and subjected to crystallization temperature of 100°C for reaction times of 6, 12, 24 and 36 hours, respectively. The samples and products were characterized using XRF, XRD, SEM and BET. The XRF analysis confirmed the status of the raw materials and gave a positive indication of the pretreatment and zeolitization processes. The highest intensity value from XRD was recorded for zeolite NaX at 24hrs reaction time, while the SEM and BET for products at 36hrs tends to be more desirable. The zeolite NaX from Kankara and Elefun obtained at 100^{0}C at 36hrs had an octahedral shape, highly crystalline in nature, having a specific surface area of about 479m^2/g and 468 m^2/g, respectively. The investigated characteristic properties tend to favorably compete with her commercial NaX (specific surface area-SSA of 423.6 m^2/g).

1. INTRODUCTION

Zeolites are a well-defined class of naturally occurring and synthetically produced crystalline aluminosilicate substances with three-dimensional structures arising from oxygen linked framework of $[SiO_4]^{4-}$ and $[AlO_4]^{5-}$ polyhedral. They are capable of facile and reversible cation exchange. The assemblages of tetrahedra create a porous matrix with regular arrays of apertures having well-defined dimensions so as to be able to selectively admit some molecules into their interiors, whilst rejecting others on the basis of molecular dimensions, giving them the important attribute of "molecular sieving." The properties of ion exchange and molecular sieving have resulted in the successful commercialization of zeolites for industry scale ammonia treatment and in detergent formulations as calcium sequestrants, and make zeolites a strong prospect for removal of heavy metals from acid mine drainage and industrial wastewaters (Breck, 1974).
Zeolite has increasingly finds a number of applications in numerous industrial processes, namely; water purification, catalyst in the petroleum refining processes, preparation of advanced materials and in nuclear reprocessing etc. Therefore, the idea of producing synthetic zeolite to continuously replace its limited natural analog cannot be overemphasized.

Zeolite X is a microporous material with a faujasite framework structure and a Si/Al molar ratio that varies from 1.0 to 1.5. Each unit cell in the three-dimensional pore system of faujasite zeolite consists of 8 supercages, 8 sodalite cages, and 16 hexagonal prisms. Zeolite X has a large pore size (7.3Å) and a high cation exchange capacity – CEC (5meq g^{-1}), which make this zeolite an interesting molecular sieve and a high-cation exchange material (Traa and Thompson, 2002). Zeolite X is receiving increased attention and currently a very attractive material for technological and environmental applications because of its prominent selective adsorption property, (Kim, 2003 and Guesmi *et al.*, 2012), high exchange capacity (Hunger *et al.*, 2000) and medium-strength basic sites. Its wide micropores make it useful for purification and separation of gases and organic components; high exchange capacity allows for adsorption of heavy cations and radionuclides (Derkowski *et al.*, 2007).

In Nigeria, many research works have been reported on the preparation and characterization of zeolites. Preliminary studies on synthesis of zeolite from local clay have been reported by Aderemi (2000), Atta (2007), Kovo (2012), Ajayi, (2012) and Ajayi (2013). Zeolites are usually synthesized from cheap silica-alumina sources in alkaline phase under hydrothermal conditions. The cheap silica-alumina sources include kaolinite. It is therefore very pertinent for researchers, engineers, to continuously investigate properties that will favour the conversion of kaolinite clay to desired zeolite, considering it application in our economy. Hence, in this research work, kaolinite clay mined from both Kankara (Katsina State) and Elefun (Ogun State) was converted using hydrothermal method into zeolite NaX while investigating the effect of crystallization time on its crystallinity.

2. METHODOLOGY AND MATERIALS

2.1 Beneficiation and Calcination of Kaolin

The clay (kaolin) samples were procured from Kankara village in Kastina State and Elefun village in Ogun State, Nigeria. Both kaolin samples were weighed and soaked in water for three days. During this period the slurries were stirred periodically (every 12 hours) after decantation of the supernatant water and addition of fresh water. The fine suspension thus obtained from each clay samples was sieved and allowed to settle. Thereafter the sediment was dried under atmospheric condition, followed by oven drying at 100^{o}C for 12 hours. The product from this stage is hereafter referred to as beneficiated Kankara kaolin (BKK) and Elefun kaolin (BEK). After drying, the beneficiated kaolin was ball milled to obtain a desired particle size. The beneficiated kaolinite clay was converted into a more reactive form - metakaolin through heating at elevated temperature of 850^{o}C in a muffle furnace for 6hours.

2.2 Dealumination

In a conical flask, 30g of metakaolin was added to 134.40ml of distilled water and 122.78ml of 96wt% H_2SO_4 (equivalent to 5-fold stoichiometric acid requirement and to form 60wt% of acid solution) to start the dealumination reaction. The reaction was driven by the thermal energy released by the acid-water mixture, with residence time set at 3 min (Ajayi *et al.,* 2010). After the set time, the reaction was quenched with 207.2ml of distilled water to bring the acid concentration to about 38wt%. The flask content was filtered through a vacuum pump filtration unit and the recovered solid was washed with deionized water in order to remove the excess acid. The de-aluminated metakaolin was dried, crushed and preserved for further application and analyses.

2.3 Gel formation and Ageing

10g of the dealuminated metakaolin (from Kankara) sample was weighed and transferred into a conical flask, where 57cm^3 of de-ionize water was introduce in batch of 35cm^3 and 22cm^3 respectively. 35cm^3 of the de-ionize water was introduce into a conical flask containing the 10g of dealuminated metakaolin sample and the mixture was agitated for about 10mins. 8.6g of the NaOH pellet was introduced under constant stirring until the mixture becomes thicker and the remaining 22cm^3 of the de-ionize water was added until a jelly like solution was noticed. The same procedure was repeated for kaolin from Elefun and the resulting gels formed were transferred into a label polypropylene bottles and aged quiescently for a period of seven days at room temperature.

2.4 Crystallization

After seven days aging, the samples in the porcelain bottles were subjected to an elevated temperature of 100^{o}C in a calibrated microwave oven. The microwave oven consumes 1,100 W AC and produces 700 W of microwave power, an efficiency of 64%, while 400 W are dissipated as heat, mostly in the magnetron tube. The reaction was made to take place at the specified temperature of 100^{o}C and time of 6hrs, 12hrs, 24hrs and 36hrs, respectively. After the synthesis, the samples were washed thoroughly with deionized water to neutrality, filtered, dried, and stored for characterization. Based on previous investigations (Ansari *et al*., 2013 and Ngoc *et al*., 2013), the crystallization temperature of 100^{0}C was chosen.

2.5 Characterization

The materials obtained at various stages were subjected to analyses, namely XRD, EDX-SEM, XRF and BET. X-Ray Fluorescence mineralogical composition of the samples was determined using a Thermo Fisher ARL9400 XP+ Sequential XRF equipped with a WinXRF software was for analyses. The samples were milled in to achieve particle sizes <75micron, dried at 100°C and roasted at 1000°C to determine Loss on Ignition (LOI) values. 1g Sample was mixed with 6g lithium tetraborate flux ($Li_2B_4O_7$) and fused at 1050°C to make a stable fused glass bead. The XRF analysis for the clay was conducted following ASTM C114 standard for oxide identification.

X-ray powder diffraction (XRD) patterns were collected on an XPERT-PRO diffractometer (PANalytical BV, Netherlands) with theta/theta geometry, operating a cobalt tube at 35 kV and 50 mA. The goniometer is equipped with automatic divergence Slit and a PW3064 spinner stage. The XRD patterns of all specimens were recorded in the 5.0°- 90° 2θ range with a step size of 0.017° and a counting time of 14 s per step. The XRD analysis was conducted following ASTM 2478, standard for clay identification, while those for zeolite NaX were conducted following ASTMD5758.

SEM and EDX analysis were recorded by using LEO S430 scanning electron microscope coupled with energy dispersive X-ray analyzer model Oxford LINK ISIS. Samples were prepared by dispersing dry powder on double sided conductive adhesive tape. Samples were coated with carbon by arc discharge method for SEM-EDX. Samples were scanned in secondary electrons (SE) for morphology and back scattered electrons (BSE) mode for compositional image.

In order to determine the specific surface area, automated gas adsorption analyzer, AUTOSORB-1 (Quanta Chrome Instruments, USA) was used with adsorption-desorption isotherms of nitrogen at -196^{0}C. For each analysis, 0.2g of sample were degassed at 300^{0}C under nitrogen for at least 3h. The specific surface areas of sample were calculated by the BET (Brunauer, Emmett, and Teller) method. The Specific surface area were determined following the standard method of ASTM C1274.

3.0 RESULTS AND DISCUSSION

3.1 Beneficiation processes-physical, thermal and chemical

The compositional analysis of the raw kaolin (Kankara and Elefun) depicted in Table 4.1 indicated that Kankara

is richer in oxides of potassium, while Elefun had a higher value for TiO_2 and both recorded similar composition for oxides of iron and magnesium. This observation was attributed to sources, location and mode of formation i.e. either potash or ferric kaolin. The effect of these inherent impurities could be noticed in the silica/alumina ratio of the starting kaolin. Theoretically, the silica/alumina ratio for pure kaolin is expected to be 2 or slightly less than 2 but not greater than 2. In this case Elefun kaolin had a relatively higher silica to alumina ratio, which might suggest level of impurities and probably incomplete formation of the kaolinite structure.

Table 1: Composition of raw, beneficiated, calcined and dealuminated kaolin

	Na_2O	MgO	Al_2O_3	SiO_2	P_2O_5	SO_3	K_2O	CaO	TiO_2	Fe_2O_3	ZnO	SrO	Si/Al
RKK	0.123	0.460	39.646	56.627	0.18	0.215	1.417	0.103	0.213	0.964	0.002	0.003	**2.42**
BKK	0.113	0.380	41.92	54.62	0.10	0.002	1.410	0.101	0.313	0.970	0.042	0.009	**2.21**
CKK	0.125	0.452	40.423	55.98	0.15	0.100	1.412	0.103	0.213	0.950	0.002	0.003	**2.35**
DKK	0.00	0.225	19.32	78.41	0.00	0.371	0.621	0.065	0.403	0.566	0.000	0.002	**6.89**
REK	0.000	0.359	30.720	60.762	0.000	0.315	0.377	0.021	4.888	1.182	0.003	0.005	**3.36**
BEK	0.103	0.480	38.92	55.62	0.00	0.301	0.360	0.001	2.313	1.170	0.022	0.003	**2.43**
CEK	0.125	0.452	40.423	54.98	0.12	0.208	0.442	0.103	0.213	0.750	0.012	0.002	**2.31**
DEK	0.00	0.199	16.91	76.30	0.00	0.363	0.363	0.077	4.958	0.828	0.000	0.002	**7.66**

Legend

RKK	Raw Kankara Kaolin	DKK	Dealuminated Kankara Kaolin	CEK	Calcined Elefun Kaolin
BKK	Beneficiated Kankara Kaolin	REK	Raw Elefun Kaolin	DEK	Dealuminated Elefun Kaolin
CKK	Calcined Kankara Kaolin	BEK	Beneficiated Elefun Kaolin		

The XRD pattern of the raw kaolin gave all the characteristic kaolinite peaks, with some peaks that can be attributed to quartz, illite, smectite, halloysite and muscovite (Figure 1). These peaks were found to conform satisfactorily to those in the open literature (Pinheiro *et al.*, 2005; Lenarda *et al.*, 2007; Panda *et al.*, 2010). The parent clay showed well defined reflections at 2Θ values of 12^0 and 30^0 (corresponding to the d values of 7.154Å; a reflection from [001]) giving typical characteristic peaks of kaolinite. The Kankara kaolin was found to contain, aside anatase, phases like potassium iron oxide and forsterite, resulting from the presence of potassium and ferric oxide in the raw kaolin. The XRD peaks were found to correlate with the XRF result as the 2Θ values of 12^0 for Elefun kaolinite clay was found to have very low intensity.

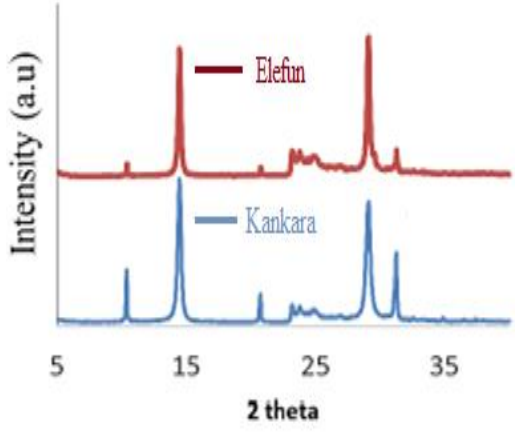

Figure 1: XRD patterns for raw Kankara and Elefun kaolinite clay.

The closely packed flaky particles are stacked together in agglomerates and seem to be predominant in both sample analyzed, as depicted in Figure 2. Noticeably small aggregate particles found in between the silica-alumina plates, under higher magnification, are indicative of inherent impurities, which are predominant in Elefun clay as shown in Figure 2 (b).

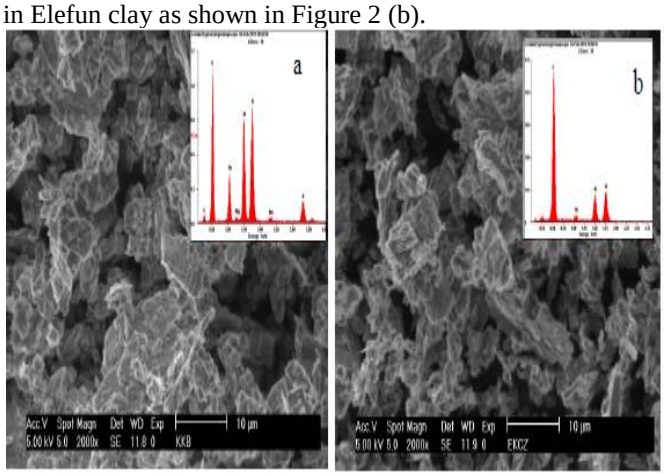

Figure 2: SEM and EDX for raw Kankara (a) and Elefun (b) kaolinite clay.

The XRD patterns of the calcined products presented in Figures 3 (a and b) are semi-amorphous in nature. The peaks for kaolinite disappeared upon thermal treatment, but it was observed that some phases were relatively passive to the thermal treatment. These observations were similar to those reported for metakaolins by other researchers (Belver *et al.*, 2002, Elimbi *et al.*, 2011). The intensity of some inherent impure phases like microcline, illite, dickite and brookite were also observed to reduce drastically with thermal treatment.

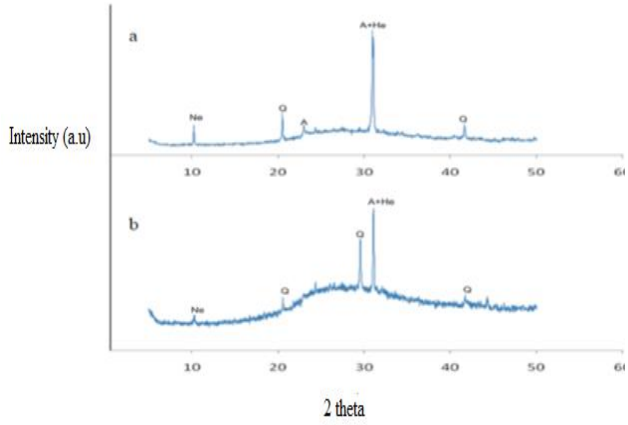

Figure 3: XRD pattern for calcined Kankara and Elefun kaolinite clay.

Figure 3b showed the XRD pattern for metakaolin obtained from Elefun kaolinite clay, with retained peaks at 2 theta around 30 and 32, attributed to the presence of quartz and hematite (Fe2O3), respectively. Those two minerals were observed to be passive to thermal treatment despite the elevated temperature of calcination, which is in agreement with the works reported by Chandrasekhar and Pramada (1999) and Lenarda *et al.*, (2007).

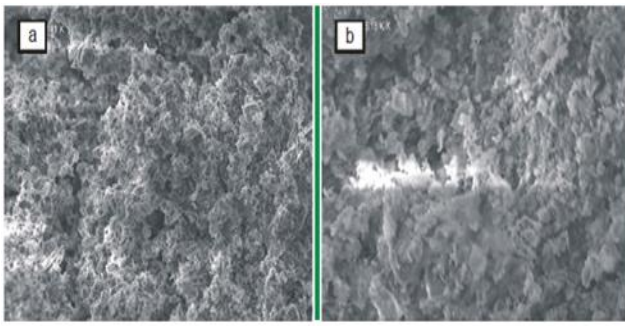

Figure 4: SEM images for calcined Kankara (a) and Elefun (b) kaolinite clay.

Figures 4(a and b) showed the SEM images for Kankara and Elefun metakaolin, respectively, obtained at calcination temperature 850^0C. The SEM images for the samples were seen to be similar, despite the source of the starting kaolin. The images gave an evidence of partial destruction of the initial kaolinite structure and formation of the semi-amorphous metakaolin, with the destruction of the noticeable card-like structure of kaolinite clay, as seen in Figure 2

The XRD patterns for the dealuminated samples pointed to the reduction of some noticeable phases after calcination and prominence of more silica rich phase with less alumina in the dealuminated sample. The intensity of these at the 2Θ around 20, 30 and 32, were more crystalline than same from the metakaolin. This tends to conforms with the chemistry of dealumination, where more silica is expected compared to alumina, for the former does not react with the acid.

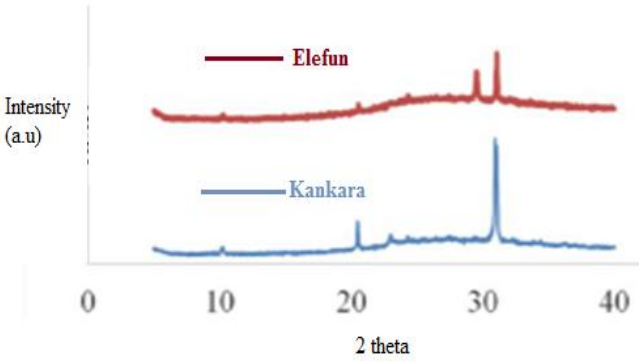

Figure 5: XRD patterns for dealuminated samples from Kankara and Elefun kaolinite clay.

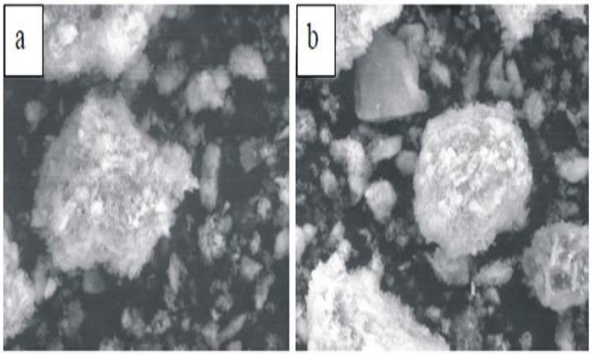

Figure 6: SEM images for dealuminated Kankara (a) and Elefun (b) kaolinite clay.

The SEM images of the dealuminated Kankara and Elefun shown in Figure 6 (a & b) indicate the disaggregation of metakaolin structure on acid treatment, resulting to surface roughness and cluster formation. The large white particles appear to be formed by several flaky particles stacked together to form well bonded agglomerates. These observations were found to favorably agree with the works reported by Lenarda *et al.,* (2007) and Panda *et al.,* (2010). Additionally, some materials remained unaffected by the acid treatment, retaining its shape from metakaolin, were noticed in the SEM for both dealuminated products.

3.2 Crystallization processes-gelation and reaction

The gels formed were observed to have closely related minerals as shown in Figure 7 (a & b), irrespective of the source of kaolinite clay used, temperature of calcination and mode of dealumination. The new phases formed namely-CIT-1, TNU-9, Go, RUB's noticed in the gels from Kankara and Elefun, testify to the action of NaOH introduced, since they are rich in sodium. The quartz peak was still noticeable in Elefun kaolinite clay. It worth mentioning, that the gel was analyzed without been subjected to aging, hence the reason for retained quartz peak in Elefun.

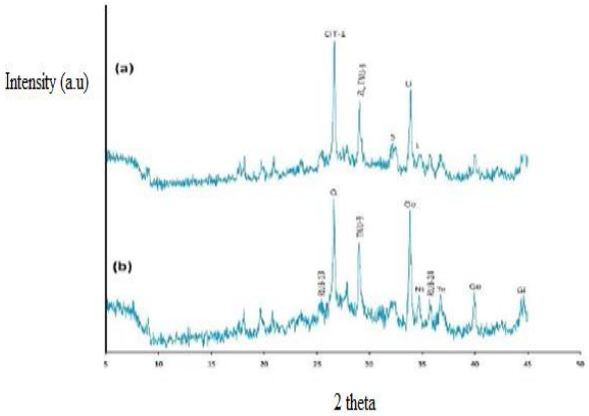

Figure 7: XRD patterns for gel produced from Kankara (a) and Elefun (b) kaolinite clay.

Conclusively, it can be inferred from the XRD patterns in Figure 7 that the gels contained disordered form of aluminosilicate in a state of higher simplexity and entropy, which is required for crystallization.

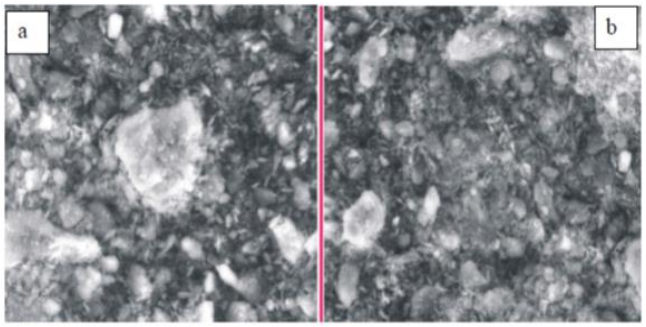

Figure 8: SEM images for gels from Kankara (a) and Elefun (b) kaolinite clay.

The SEM image actually correlates the aforementioned speculation as shown in Figures 8(a & b), where the bulky though flaky particle observed in the figures were noticed to have broken down into smaller closely packed particles. The gel obtained from Kankara was observed to retain a relatively large portion of the flaky but bulky particle, embedded in amorphous aggregates, suggesting its compositional resistance to alkaline treatment.

The XRD patterns of all the as-synthesized zeolite NaX exhibit diffraction peaks which are characteristic of NaX zeolite. It was observed from Figures 9-12, that increase in crystallization time resulted in enhanced crystallinity and crystal size of zeolites.

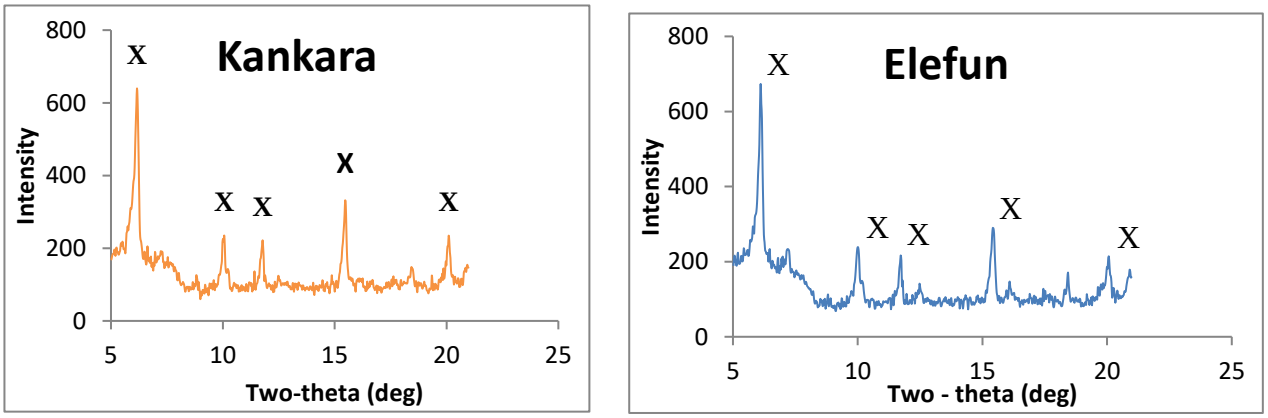

Figure 9: XRD patterns for crystallized product at 6 hours

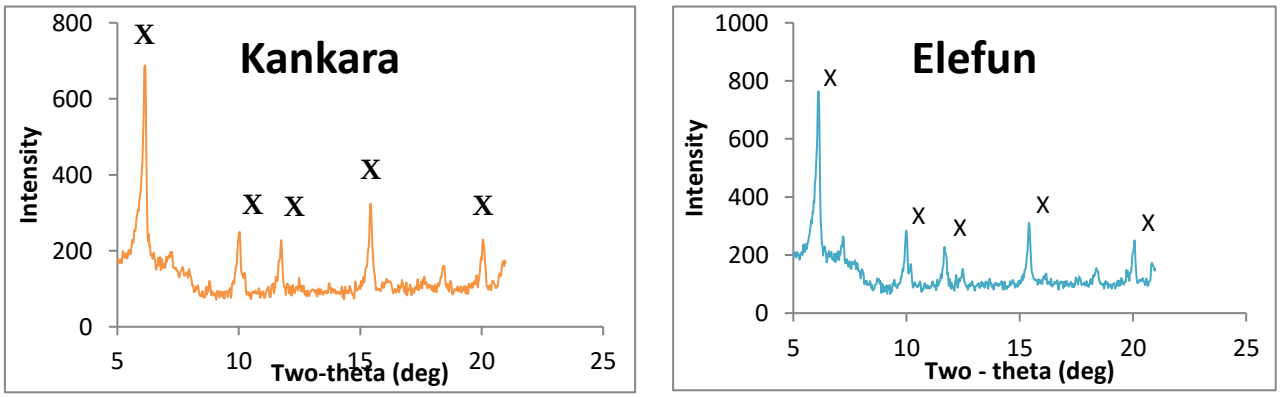

Figure 10: XRD patterns for crystallized product at 12 hours

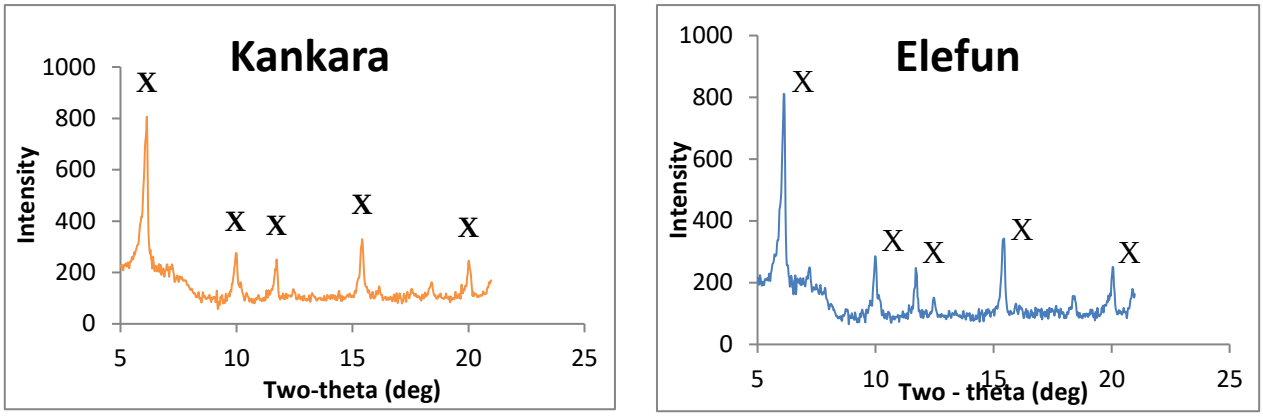

Figure 11: XRD patterns for crystallized product Sample of 24 hours

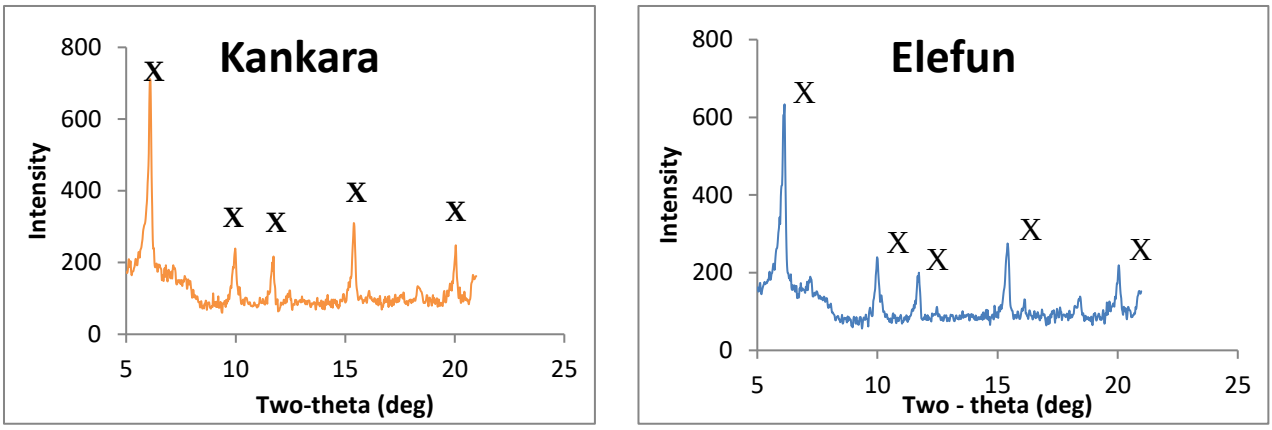

Figure 12: XRD patterns for crystallized product Sample of 36 hours

The intensity (by XRD) increased sharply with increase in crystallization time from 6 to 24hrs and then starts to decrease with time. It is speculated that the crystal phase already formed can be broken down into silica and alumina which might lead to the regrouping of the siliceous bond (formation of siloxane bridges) hence a rather more stable α-quartz phase. This can be noticed for both kaolinite clays sources, for the intensity for the major peak was observed to drop.

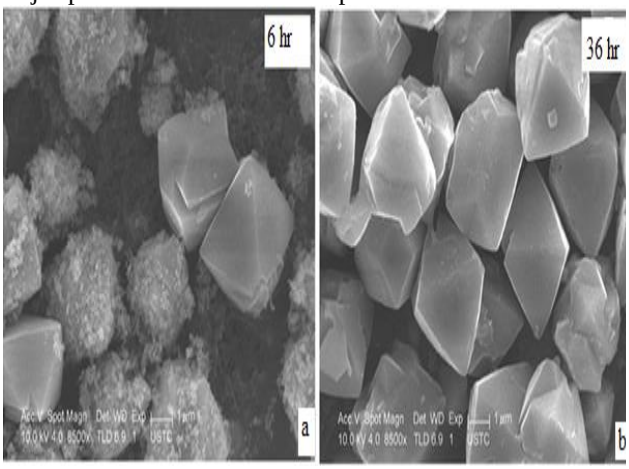

Figure 13: SEM images for Kankara based NaX zeolite crystallized for 6hr and 36hr

The SEM for NaX from kaolin and Elefun at crystallization time of 6 and 24hrs are shown in Figures 13 and 14, respectively. Figure 13a, shows the appearance of octahedron shape corresponding to NaX but with rough unsmooth edges surrounded by rather amorphous like materials, suggesting incomplete conversion/crystallization process. This observation was not seen in the better and more refined shape obtained at 36hrs (see Fig 13b). Same observation was noticed for Elefun as depicted in Figure 14 but with better morphology for NaX obtained at 6hrs and less amorphous unconverted materials.

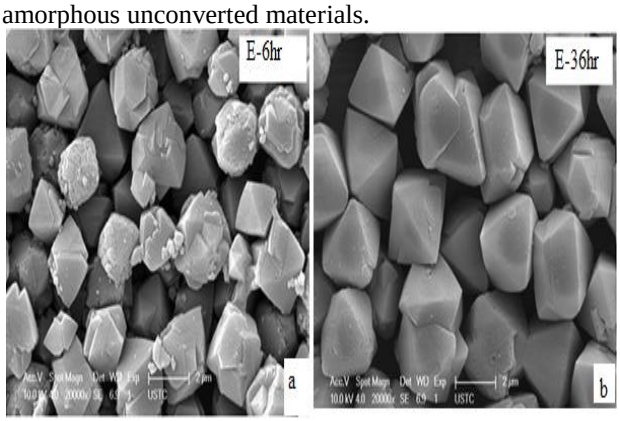

Figure 14: SEM images for Elefun based NaX zeolite crystallized for 6hr and 36hr

Figure 15 shows the values of specific surface area (SSA) for all samples and the NaX produced from it. The SSA for the raw kaolinite clays was observed to be very close in value, as well as that for the beneficiated and calcined samples. This reduction in the surface area for metakaolin is likely the result of aggregation of particles when structural water molecules were removed. The SSA for the dealuminated sample was observed to increased drastically due to the removal of alumina and enrichment of silica content, as also discussed by Belver *et al.*, (2002). The relatively high surface area observed for the dealuminated sample served as an enhancement factor for gel formation, by providing the surface area required for the gelation and subsequent crystallization. Introduction of NaOH during gel formation reduces the inherent SSA.

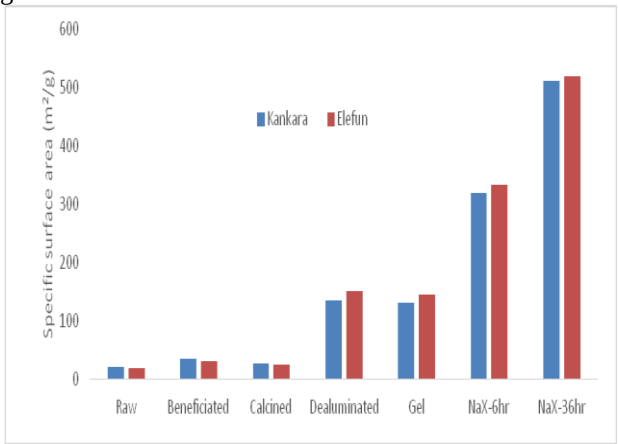

Figure 15: Specific surface area of all the samples and products

This high value of surface area is required in order to: (i) reduce the level of segregation between the reacting species and (ii) enhance the reaction rate via availability of large surface area. Also, Belver *et al.*, (2002), reported that the crystalline
nature of the gel formed in their work had large particle size, responsible for the lowered surface
area. The BET surface area for the as-synthesized zeolite was recorded to be attain a value of about 310 and 330m^2/g for NaX obtained at 6hrs crystallization reaction time and over 450m^2/g for both Kankara and Elefun, respectively at crystallization time of 36hrs. This is so probably because at low crystallinity, the SSA are reduced due to amorphous aluminosilicate blockage of the external pores of zeolite crystals, which tends to be freed at increased crystallization time, hence higher SSA (Ansari *et al.*, 2013) The SSA for NaX at 36hrs conforms with the value from the literature, of 423.6m^2/g (Schimidt *et al.*, 2013).

4. CONCLUSIONS

Zeolite NaX was successfully synthesized from kaolinite clays sourced from Kankara and Elefun, despite their inherent impurities. Both clays were subjected to beneficiation processes to improve on the property of the starting material. The zeolitization processes was conducted at 1000C at varied crystallization reaction times of 6, 12, 24 and 36hrs, respectively. Zeolite NaX produced at 36hrs were observed to have closer property to their commercial counterpart despite their low intensity compared with those from 24hrs. XRD, SEM, XRF and BET analytical techniques were employed to characterized the raw materials and resulting products. It can be concluded that both clay can serve as good

source for zeolite NaX synthesis, but with preference for Elefun kaolinite clay.

REFERENCES

Aderemi, B. O. (2000). Development of zeolite cracking catalyst from local raw materials, *Ph.D Thesis, ABU, Zaria*.

Atta, A.Y., Ajayi, O.A. and Adefila, S.S (2007). Synthesis of Faujasite Zeolites from Kankara Kaolin *Clay.Journal of Applied Sciences Research*, 3(10): 1017-1021.

Ajayi, O.A., A.Y Atta, B.O. Aderemi, A. S. Ahmed, M.T. Ityokumbul and S. S.Adefila (2012) Synthesis of Zeolite ZSM3 from Faujasite: Effects of Post-synthesis Ageing and *Insitu seeding*. *Chemical and Process Engineering Research* Vol 3, 29-39.

Ajayi, A.O., Atta, A.Y., Aderemi, B.O. and Adefila, S.S. (2010). Novel Method of Metakaolin Dealumination - Preliminary Investigation. *Journal of Applied Sciences Research*, 6(10): 1539-1546.

Ajayi, O. A., Adefila, S. S., Ityokumbul, M. T. (2017). Monitoring zeolite NaY formation from potassium-rich Nigerian kaolinite clay. *Ain Shams Engineering Journal.*

Ansari, M., A. Aroujalian, A. Raisi, Dabir, B. and M. Fathizadeh (2013). Preparation and characterization of nano-NaX zeolite by microwave assisted hydrothermal method. *Advanced Powder Technology*. ttp://dx.doi.org/10.1016/j.apt.2013.10.021.

Belver, C., M.A.B. Munoz and M.A. Vicente (2002). Chemical Activation of a Kaolinite under Acid and Alkaline Conditions. *Chemical Material*. 14: 2033-2043.

Breck, D. W. (1964). Crystalline molecular sieves. *Journal of Chemical Education*, 41 (12), 678-689.

Chandrasekhar, S. and P.N. Pramada (2004). Kaolin-Based Zeolite Y, a Precursor for Cordierite Ceramics, *Applied Clay Science*, 27(3): 187-198.

Derkowski, A., W. Franus, H. W-Nowicka, A. Czimerova (2007). "Textural properties vs. CEC and EGME retention of Na–X zeolite prepared from fly ash at room temperature", *Int. J. Miner. Process.*, vol. 82, 57- 68.

Elimbi, A., H.K. Tchakoute, D. Njopwouo (2011). Effects of calcination temperature of kaolinite clays on the properties of geopolymer cements. *Construction and Building Materials*, Volume 25, Issue 6, 2805-2812

Guesmi H, Massiani P, Nouali H, Paillaud J.L.(2012). A combined experimental and theoretical study of the simultaneous occupation of SIa and SI′ sites in fully dehydrated K-LSX *Microporous and Mesoporous Materials*. 159: 87-95. DOI: 10.1016/j.micromeso.2012.04.011

Hunger, M; Schenk, U; Seiler, M; Weitkamp, J (2000). In situ MAS NMR spectroscopy of surface compounds formed from methanol and from a toluene/methanol mixture on basic zeolite X. J of Molecular Catalysis A: Chemical ISSN: *1381-1169* Vol.156 Issue 1-2 153-161

Kim, Jin-Bae (2003). Li^+- and H^+-Exchanged Low-Silica X Zeolite as Selective Nitrogen Adsorbent for Air Separation. *Bulletin of the Korean Chemical Society*, volume 24, issue 12, 2003, Pages 1814-1818. DOI : 10.5012/bkcs.2003.24.12.1814

Kovo, A.S.(2012). Effect of Temperature on The Synthesis of Zeolite X from Ahoko Nigerian Kaolin Using Novel Metakaolinization Technique. Journal of Chemical Engineering Communications, Volume 199, 2012 - Issue 6 Pages 786-797. http://dx.doi.org/10.1080/00986445.2011.625065

Ngoc, D.T., T. H. Pham and K.D. H. Nguyen (2013). Synthesis, characterization and application of nanozeolite NaX from Vietnamese kaolin. Adv. Nat. Sci.: Nanosci. Nanotechnol. 4 045018 (12pp) doi:10.1088/2043-6262/4/4/045018

Lenarda, M., L.Storaro, Talon, A., E.Moretti and Riello, P (2007). Solid acid catalysts from clays: Preparation of mesoporous catalysts by chemical activation of metakaolin under acid conditions. *Journal of Colloid and Interface Science* 311, 537-543

Panda, A. K., B.G. Mishra, D.K. Mishra, R.K. Singh (2010). Effect of sulphuric acid treatment on the physico-chemical characteristics of kaolin clay. *Colloids and Surfaces A: Physicochemical and Engineering Aspects*. Vol.363, Issues 1–3, 98–104

Pinheiro, P.G., J.D. Fabris, Mussel, W.N., E. Murad, Scovzelli, R.B. and V.K.Garg (2005). Beneficiation of a commercial kaolin from Mar de Espanha, Minas Gerais, Brazil: Chemistry and Mineralogy. *Journal of South American Earth Sciences* 20, 267-271

Schimidt, T. M. P., F. R. Soares, V. Slusarski-Santana, F. F. Brites-Nóbrega and N. R. C. Fernandes-Machado (2013). Chapter 99. Photocatalytic degradation of textile effluent using ZnO/NaX and ZnO/AC under solar radiation. Green Design, Materials and Manufacturing Processes. Edited by Telma Ferreira, CRC *Press, Taylor and Francis Group, London.* pp 563–566. https://doi.org/10.1201/b15002-109

Traa, Y. and Thompson, R.W. (2002) Controlled Co-Crystallization of Zeolites A and X. *Journal of Materials Chemistry*, 12, 496-499. http://dx.doi.org/10.1039/b108634k